DEVELOPMENT OF STATE-OF-CHARGE OBSERVERS FOR LEAD-ACID STORAGE UNITS FOR SOLAR-ASSISTED AUTONOMOUS APPLICATIONS

Alexandre Skrylnyk, Renato Lepore, Marcel Remy and Marc Frère

Energy Research Centre, University of Mons, bd. Dolez 31, 7000 Mons (Belgium)

1. Introduction

Electric energy storage is a crucial problem for autonomous systems powered by photovoltaic installations. The excess of produced energy under favourable conditions is normally stored into batteries. For large scale applications, where more than one battery is used, the correct utilization of the storing bank plays an important role in order to extend the batteries' lifetime. The context of this work is related to the research on a solar assisted domestic heating application, which includes an autonomous photovoltaic installation and a software-driven resistance load which represents a dwelling heated by a heat pump. The load stands as a sink with time-varying energy consumption. The energy pattern resulting from the climate condition and the user driving behaviour implies a hard float cycling work of the storing bank. Moreover, in such applications, due to the tolerances on the internal parameters, the interactions between the batteries are unavoidable. As a result, some storage units work under constant discharge conditions whereas the others take on the overcharge current and imbalances occur. Therefore, a state-of-charge monitoring scheme of an individual unit can provide an essential information in order to improve energy management.

The notion of State-Of-Charge (SOC) can be explained in terms of the energy available to the user in given charge/discharge conditions. Knowing the amount of energy left in a battery compared with the energy it had when it was new gives the user an indication of how much longer a battery will continue to perform before it needs recharging. The SOC is a fictitious variable which embodies the physical phenomena that occur in the battery and it cannot be explicitly measured. Hence, many modelling approaches have been developed to determine the SOC (Jossen et al., 2001; Sabatier et al., 2006; Rodrigues et al., 2000; Sauer, 1997). Unfortunately, none of the existent model assures a reliable estimation of it and new approaches are under development. Typically, the procedure of SOC determination involves the modelling of the battery behaviour under operating conditions. Generally, several methods of SOC estimation are used:

- SOC as a linear/non-linear function of the battery open circuit voltage.
- Ampere-counting techniques such as current integration.
- SOC as a function of the battery impedance.

Each technique has its disadvantages. Since the SOC is a non-linear function depending on many parameters it is difficult to design an adequate model. The open circuit voltage represents the SOC function but is not though available under load. Thus, different observers based on the equivalent electric circuit have been designed to reconstruct this state in order to determine the SOC.

The current integration method stands as a better solution to determine the SOC and it takes into account all charging and discharging currents. But also ampere counting does not allow an adequate SOC processing due to the errors accumulated during integration.

The Electrochemical Impedance Spectroscopy (EIS) methods (Rodrigues et al., 2000) are commonly used to determine the physical parameters of the equivalent electric circuit and therefore give the essential information about SOC. Nevertheless, the battery impedance does not altogether reflect the SOC but provides in turn knowledge about faults, battery age, corrosion of electrodes, and other active mass properties. Besides, its practical implementation with systems that constantly work under load is complicated too.

Since the battery exhibits a non-linear behaviour and its parameters may contain uncertainties, it appears interesting to study and compare two approaches of SOC calculation:

- robust state estimation, based on the sliding mode technique;
- fuzzy logic observation, based on the black-box modelling.

The sliding mode technique for SOC calculation is an important approach for robust observers design. It addresses the problem to improve the accuracy of information of incoming data containing errors or uncertainties (Utkin, 1978; Barbot et al., 2002). The recent investigations in SOC estimation for lithium batteries (Kim, 2006) prove the interest of developing robust observers also for other types of electrochemical storage units. However, the gain of robustness properties pays its price for some speed performances.

The fuzzy logic approach stands as a very promising technique to estimate the SOC based on the least knowledge about the battery behaviour. Fuzzy logic allows complex systems to be modelled using a higher level of abstraction originating from knowledge and experience. To observe the SOC, the novel researches in this direction exhibit good results. Numerous papers describe fuzzy logic observers which use the impedance knowledge database to determine the SOC (Raisner et al., 1990; Raisner et al., 2004). However, the implementation of such observers is rather complicated because of the impedance measuring scheme. In practice only two parameters are available - voltage and current. Since the current-based SOC estimation method provides higher accuracy but still needs compensation for the operating conditions, it can be combined with the voltage-based method.

The organization of this work as follows. Section 2 describes the experimental part and the equipment nomenclature. The development issues are reported in section 3. Finally, the main results are exposed and discussed in the section 4. Some theoretical issues and numerical values are annexed.

2. Experimental

The experimental data have been collected from a flooded-vented lead-acid battery with declared 125 Ah of capacity for 20 h and 12 V of nominal operating voltage. The battery (VARTA) is designed to work in float cycling regime. The battery has been integrated into an experimental installation that consisted of a constant-voltage power supply (Agilent 6268B) connected to a battery charge regulator (STECA TAROM 2140) equipped with a data logger (TarCom). A programmable electronic load (KIKUSUI PLZ-4W) has been either used to determine the energy consumption profile. The charge regulator has a built-in SOC meter and the manufacturer states its high reliability.

Two kinds of experiments have been carried out.

a) Impulse current discharge test. It allowed obtaining explicitly the analytical dependency of the open circuit voltage to the SOC. The applied procedure comprised the alternating short discharging tests with a 12.5A current and 10-minute rest periods. Both the open circuit voltage and the SOC then have been recorded in the data logger at the end of every rest period.

b) Sequential charge and discharge test. It has aimed to investigate the battery behaviour in different discharging and charging conditions. The initially fully charged battery has been subjected to discharging and charging cycles of 1A-, 3A-, 5A-, 7A-, 9A- and 11A-constant rate current. The measurements of voltage, current and SOC have been stored in the data logger during 333 hours of total work.

All the experiments have been carried out in a protected ambiance at about 20 °C without significant temperature variations - less than 1 °C.

3. State-of-charge observers design

3.1. Robust sliding-mode observer

A robust observer faces the state estimation problem out of very inaccurate information. In real operating conditions, the battery is influenced by unknown disturbances and the model parameters vary with time. The sliding mode technique guarantees the robustness of the observer as it allows rejecting any parameter variation and any unpredictable disturbance.

3.1.1. System modelling

The structure of the sliding mode observer is based on the RC-equivalent electric circuit presented in figure 1, that many researchers have used to model the behaviour of an electrochemical storage unit (Sutano et al., 1995).

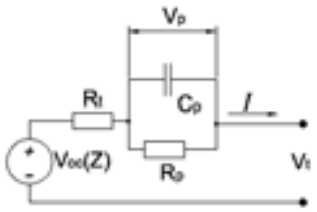

Fig. 1: RC-equivalent electric circuit of a lead-acid battery

The source $V_{oc}(Z)$ depends on the SOC, denoted as Z. R_t is the internal resistance of the battery, R_p is the charge transfer resistance which is due to limitations in the chemical reaction rates at the electrode/electrolyte side, C_p is the polarization capacitance. Both R_p and C_p are used to model the diffusion phenomena and the repartition of the cumulated charge in the active mass.

The numerical values of parameters R_t, R_p ad a C_p are usually identified by the EIS method with some adequate equipment. Numerous papers contain results of the EIS identification for lead-acid batteries (Gopikanth et al., 1979; Viswanatan et al., 1994). Since the systems designed on the ground of the sliding mode theory exhibit robustness properties in the face of internal parameters variations, we suggest to use as numerical values of parameters those which are cited in the literature (Gopikanth et al., 1979; Viswanatan et al., 1994).

In accordance with the impulse current discharge test *(a)* results, the open circuit voltage $V_{oc}(Z)$ has been modelled by using a nonlinear function:

$$V_{oc}(Z) = kZ + d - \mu_1 e^{-\mu_2 Z} \quad \text{(eq. 1)}$$

The comparison of the measured and approximated open circuit voltages is shown in figure 2. The time derivative of the SOC is defined as follows:

$$\dot{Z} = \frac{I}{C_N} \quad \text{(eq. 2)}$$

where C_N is the rated capacity and I is the sum of all currents coming in or out of the battery. As noted in figure 1, the output voltage is the sum of the open circuit voltage $V_{oc}(Z)$, of the drop of voltage in the internal resistance R_t and of the polarization voltage V_p:

$$V_t = V_{oc}(Z) + R_t I + V_p \quad \text{(eq. 3)}$$

The dynamic of the polarization voltage V_p is governed by the following equation:

$$\dot{V}_p = -\frac{1}{R_p C_p} V_p + \frac{I}{C_p} \quad \text{(eq. 4)}$$

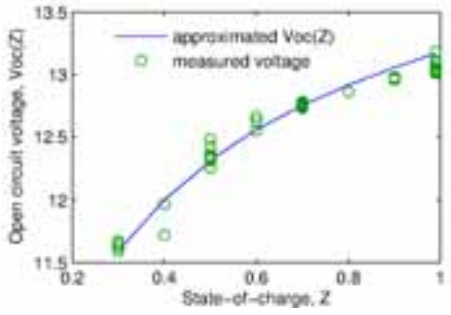

Fig. 2: Measured and approximated open circuit voltages

By replacing $V_{oc}(Z)$ in (3) with (1), the state equation system writes as follows:

$$\begin{aligned} \dot{Z} &= \frac{I}{C_N} \\ \dot{V}_p &= -\frac{1}{R_p C_p} V_p + \frac{I}{C_p} \end{aligned} \quad \text{(eq. 5)}$$

$$V_{\mathrm{t}} = kZ + V_{\mathrm{p}} + d - \mu_1 \mathrm{e}^{-\mu_2 Z} + R_{\mathrm{t}} I$$

By denoting the values $b_1 = 1/C_{\mathrm{N}}$; $b_2 = 1/C_{\mathrm{p}}$; $a_{22} = -1/(R_{\mathrm{p}} C_{\mathrm{p}})$; $c_1 = k$; $d_1 = R_{\mathrm{t}}$; $\varphi(x) = d - \mu_1 \mathrm{e}^{-\mu_2 Z}$; $x_1 = Z; x_2 = V_{\mathrm{p}}$; $y = V_{\mathrm{t}}$; $u = I$ and successively:

$A = \begin{bmatrix} 0 & 0 \\ 0 & a_{22} \end{bmatrix}$; $B = \begin{bmatrix} b_1 \\ b_2 \end{bmatrix}$; $C = [c_1 \quad 1]$; $D = d_1$, $x = [x_1 \quad x_2]^T$, equations (5) are rewritten in canonical representation:

$$\begin{aligned} \dot{x} &= Ax + Bu \\ y &= Cx + Du + \varphi(x) \end{aligned} \qquad \text{(eq. 6)}$$

3.1.2. Observer design

The observer designed for system (6) is described as:

$$\begin{aligned} \dot{\hat{x}} &= A\hat{x} + Bu + L(y - \hat{y}) + \psi(\hat{x}, y, \tilde{y}) \\ \hat{y} &= C\hat{x} + Du + \varphi(\hat{x}) \end{aligned} \qquad \text{(eq. 7)}$$

where L is a linear gain vector and $\psi(\hat{x}, y, \tilde{y}) \in \mathbb{R}$ is a non-linear correction term whose properties will be discussed later. It should be noted that the spectrum of matrix A is located in the left half-plane, so that spectrum $\lambda(A) \leq 0$. The output error is defined as follows:

$$\begin{aligned} \tilde{y} &= y - \hat{y} \\ \tilde{y} &= C\tilde{x} + \delta(x_1, \tilde{x}_1) \end{aligned} \qquad \text{(eq. 8)}$$

where $\tilde{x} = x - \hat{x}$ is the state error and $\delta(x_1, \tilde{x}_1)$ is the non-linear output error. One can see that the non-linear output error is the difference $\varphi(x) - \varphi(\hat{x})$ and using relation $\hat{x}_1 = x_1 - \tilde{x}_1$:

$$\delta(x_1, \tilde{x}_1) = \mu_1 \mathrm{e}^{-\mu_2 x_1} (\mathrm{e}^{\mu_2 \tilde{x}_1} - 1) \qquad \text{(eq. 9)}$$

Since the exponential function is used, the non-linearity $\delta(x_1, \tilde{x}_1)$ is bounded by sector $[0, \infty]$ and always remains of the positive sign for all $x_1 \in [0,1]$. In this case, the observability of (6) can be verified using criteria for the linear time invariant systems. The system is observable as the rank of observability matrix is equal to system's order:

$$\mathcal{O}_n = \begin{bmatrix} C \\ CA \end{bmatrix} = \begin{bmatrix} c_1 & 1 \\ 0 & a_{22} \end{bmatrix}; \ \mathrm{rank}(\mathcal{O}_n) = 2$$

According to the weaker observability condition, the non-linear state error function converges to zero as the linear state error $\tilde{x}_1$ tends to zero:

$$\lim_{t \to \infty} \tilde{x}_1(t) = 0 \Rightarrow \lim_{t \to \infty} \delta(x_1, \tilde{x}_1, t) = 0 \qquad \text{(eq. 10)}$$

One proves the stability of the observer as follows. Consider a Lyapunov candidate function:

$$V = \tilde{x}^T P \tilde{x} \qquad \text{(eq. 11)}$$

whose time derivative must be negative or equal to zero:

$$\dot{V} = \dot{\tilde{x}}^T P \tilde{x} + \tilde{x}^T P^T \dot{\tilde{x}} \leq 0 \qquad \text{(eq. 12)}$$

where P is a positive definite symmetric matrix ($P = P^T > 0$). The derivative of $\tilde{x}$ can be found by differentiating the difference:

$$\dot{\tilde{x}} = \dot{x} - \dot{\hat{x}} = (A - LC)\tilde{x} - L\delta(x_1, \tilde{x}_1) - \psi(\hat{x}, y, \tilde{y}) \qquad \text{(eq. 13)}$$

where L is such that the system (A, C) is stable. A further calculation yields:

$$\begin{aligned} \dot{V} &= \big((A - LC)\tilde{x} - L\delta(x_1, \tilde{x}_1) - \psi(\hat{x}, y, \tilde{y})\big)^T P\tilde{x} + \tilde{x}^T P^T \big((A - LC)\tilde{x} - L\delta(x_1, \tilde{x}_1) - \psi(\hat{x}, y, \tilde{y})\big) = \\ &= \tilde{x}^T \big((A - LC)^T P + P^T (A - LC)\big)\tilde{x} - 2\tilde{x}^T P^T \big(L\delta(x_1, \tilde{x}_1) + \psi(\hat{x}, y, \tilde{y})\big) \leq 0 \end{aligned} \qquad \text{(eq. 14)}$$

Since (A, C) is stable, the first term is negative, so condition (14) will hold if the second term is negative for any $\tilde{x}$. $\tilde{x}^T P^T L\delta(x_1, \tilde{x}_1) \geq 0$ holds if and only if there exists such a positive constant $f_1 > 0$, so that $\tilde{x}^T P^T L = f_1 \tilde{x}_1, \forall \tilde{x}_1$. This statement is possible since the non-linearity belongs to the class of monotonic functions bounded in sector $[0, \infty]$. Defining $F = [f_1 \quad 0]$, $F = L^T P$, the following linear matrix inequality (LMI) problem has a solution into F and P:

$$A^T P + P^T A - C^T F - F^T C < 0 \quad \text{(eq. 15)}$$

Finally, the linear gain can be calculated as follows:

$$L = P^{-1} F^T \quad \text{(eq. 16)}$$

The procedure of LMI verification is presented in appendix A.1. The non-linear correction term can be chosen as $\psi(\hat{x}, y, \tilde{y}) = G\psi_1(\tilde{y})$, where $G \in \mathbb{R}^{n \times m}$ is the gain matrix. Basing on the stability approach for the Lur'e systems with generalized sector condition (Hu et al., 2004), it can be shown that the term $\tilde{x}^T P^T \psi(\hat{x}, y, \tilde{y})$ remains also positive, if:

$$\tilde{x}^T P^T \big((A - LC)\tilde{x} - G\psi_1(\tilde{y})\big) < 0, \forall \tilde{x} \in \mathcal{D} \quad \text{(eq. 17)}$$

with $\mathcal{D}$ that represents some contractively invariant ellipsoid. We assume that $\psi_1(\tilde{y})$ is a concave odd function, which satisfies the property $\psi_1(-\tilde{y}) = -\psi_1(\tilde{y})$ and for which exists a set of inclusions $\psi_1(\tilde{y}) \in \text{co}\{\rho_0 C\tilde{x}, \dots, \rho_i C\tilde{x}, \dots \rho_N C\tilde{x}\}$, $0 > \rho_0 > \rho_i$, $\forall i = 1 \dots N$. Since the $\psi_1(\tilde{y})$ is concave, the following inequalities hold for all $\tilde{x} \in \mathcal{D}$:

$$\begin{gathered} \rho_i C\tilde{x} \le \psi_1(\tilde{y}) \le \rho_0 C\tilde{x}, \qquad \text{if } \tilde{x} > 0 \\ \rho_0 C\tilde{x} \le \psi_1(\tilde{y}) \le \rho_i C\tilde{x}, \qquad \text{if } \tilde{x} < 0 \\ |\tilde{y}| < \varepsilon_i, \forall i = 1 \dots N \end{gathered}$$

Therefore, statement (17) yields:

$$\tilde{x}^T P^T \big((A - LC)\tilde{x} - G\psi_1(\tilde{y})\big) \le \max\big\{\tilde{x}^T P^T \big((A - LC) - \rho_0 GC\big)\tilde{x},\ \tilde{x}^T P^T \big((A - LC) - \rho_i GC\big)\tilde{x}\big\} < 0$$

It is obvious that this condition holds, *iff*

$$G = P^{-1} C^T \quad \text{(eq. 18)}$$

Hence, the observer is asymptotically stable.

3.2. Model free fuzzy logic observer

The structure of the fuzzy logic observer relies on the corresponding fuzzy logic controller, of the type Takagi-Sugeno. The synthesis of the fuzzy logic observer is achieved within two stages:

- Choice of the observer's structure;
- Tuning of the observer's parameters.

3.2.1. Choice of the structure

Since the fuzzy logic method refers to "black-box" modelling, the decision making rule may a priori include explanatory variables without really physical interpretation in the studied process. For example, one can assume that the variation of the SOC depends on a linear combination of the instantaneous current $I(t)$, voltage $V_t(t)$ and actual SOC $Z(t)$ (Jossen et al., 2001). However, by applying the notion of energy, the modified relation is introduced in this work:

$$Z(t) = E(t) - W(t) \quad \text{(eq. 19)}$$

This relation is interpreted: the available energy $Z(t)$ at time t is equal to the difference of the work $E(t)$ that potentially could be done for given charging/discharging conditions, with specified $V_t(t)$, and the overall work that is done $W(t)$. Considering $W(t) = \theta_1 \int_0^t I(\tau) d\tau$ and $E(t) = \theta_0 + \theta_2 V_t(t)$, the relation (19) can be rewritten in the following form:

$$Z(t) = \theta_0 - \theta_1 \int_0^t I(\tau)\, d\tau + \theta_2 V_t(t) \quad \text{(eq. 20)}$$

Thus the explanatory variables are chosen as $x_1 = \int_0^t I(\tau) d\tau$ and $x_2 = V_t(t)$ for the output mapping $y = Z(t)$ and like parameters θ_0, θ_1 and θ_2 are to identify. The structure of the observer is determined by specifying the inputs $X = \{x_1, x_2\}$, their values $\forall x_i \in A_i$, $A_i = \{a_{i,1}, a_{i,2}, \dots, a_{i,N}\}$, $1 \le i \le |X|$, the output mapping $F: X \to y$, and the number of fuzzy rules N. The decision making rule is designed as follows:

$$y = \theta_0 - \theta_1 x_1 + \theta_2 x_2 \quad \text{(eq. 21)}$$

The fuzzy logic resolution scheme can be expressed in the form of Takagi-Sugeno rules (Babuska et al., 1996):

$$\text{if } x_1 \in A_1 \wedge x_2 \in A_2 \text{ then } F: X \to y \quad \text{(eq. 22)}$$

With:

$$A_i = \{a_{i,j}\}_{\substack{1 \le i \le |X| \\ 1 \le j \le N}}, F = \{f_j(X)\}_{1 \le j \le N} \quad \text{(eq. 23)}$$
$$f_j(X) = \theta_{0,j} - \theta_{1,j}x_1 + \theta_{2,j}x_2$$

Therefore, the estimated output is equal to:

$$\hat{y} = \frac{\sum_{j=1}^{N} w_j \cdot f_j(X)}{\sum_{j=1}^{N} w_j} \quad \text{(eq. 23)}$$
$$w_j = \prod_{i=1}^{|X|} \mu_{i,j}(x_i), 1 \le j \le N$$

The fuzzy rules are obtained within two steps. In the first step, the vector of measured data (X, y), which has been obtained from the sequential charge and discharge test *(b)*, is subjected to the fuzzy clustering procedure (Dunn, 1973) in order to map hyperboxes embedding every cluster $U_j \supset \{(X', y')_j, \dots (X'', y'')_j\}$, with $(X', y')_j \cup \dots (X'', y'')_j \subseteq (X, y)$. In the second step, the set of hyperboxes $U = \{U_j\}_{1 \le j \le N}$ is converted into the set of membership functions $\{\mu_{i,1}(x_i), \mu_{i,2}(x_i), \dots \mu_{i,N}(x_i)\}, 1 \le i \le |X|$ by projecting each cluster onto X.

3.2.2. Tuning of the parameters

During this stage of design, firstly the vector of unknown output parameters is found $\Theta_j = [\theta_{0,j} \quad \theta_{1,j} \quad \theta_{2,j}]$, $1 \le j \le N$. For each fuzzy rule specified with (22), the vector of unknown parameters is calculated using the least-squares approach (Soderstrom et al., 1988):

$$\Theta_j = \left(X_e^T W_j X_e\right)^{-1} X_e^T W_j \cdot y \quad \text{(eq. 24)}$$

with vector $X_e = [\mathbf{1} \quad X]$, matrix $W_j = \text{diag}(U_j)$ and measured output y. Secondly, the set of input parameters for membership functions $\mu_{i,j}(x_i)$ is identified. The Gaussian representation of the membership function is suggested for all input terms:

$$\mu_{i,j}(x_i) = e^{-\left(\frac{x_i - c_{i,j}}{b_{i,j}}\right)^2}, 1 \le i \le |X|, 1 \le j \le N \quad \text{(eq. 25)}$$

The learning algorithm has been designed to adjust the set of unknown parameters $(b_{i,j}, c_{i,j})$. The applied algorithm is based on an evolutionary programming technique (Rechenberg, 2000) which uses the high-level vector coding of solution $S = [h_1 \quad h_2 \quad \cdots \quad h_j \quad \cdots \quad h_N]$, with $h_j = [b_{i,j} \quad c_{i,j} \quad b_{i+1,j} \quad c_{i+1,j}]$. First, the algorithm generates the set of possible solutions $\{S_r\}_{1 \le r \le N_p}$. The selection of the best solution performs iteratively by calculating the fitness function for each vector of solutions:

$$\min FF(S_r) = \|y - \hat{y}(S_r)\| \quad \text{(eq. 26)}$$

The solution is accepted if the fitness function tends to a minimum. In order to diversify the region of the optimal solution research and not to let the algorithm stagnate at a local optimum, the so-called "crossover" and "mutation" operations have been used. The crossover operation performs between two pairs of vectors S_r and S_k, which are the candidates for the optimal solution. It consists in recombining the internal terms h_j, so that two new vectors Sch_r and Sch_k are created:

$$h_j^{Sch_r} = \begin{cases} h_j^{S_r}, & \text{if } j < z_c \\ h_j^{S_k}, & \text{if } j \ge z_c \end{cases}, h_j^{Sch_k} = \begin{cases} h_j^{S_k}, & \text{if } j < z_c \\ h_j^{S_r}, & \text{if } j \ge z_c \end{cases} \quad \text{(eq. 27)}$$

where z_c is the random number specifying the recombination point. The mutation operation brings the alterations to some values of the new set of vectors $\{S_r \cup Sch_r\}_{1 \le r \le N_p(1+p_c)}$ in accordance with the normal distribution law $\mathcal{N}(\cdot)$:

$$h_j = \left[\mathcal{N}\left(\frac{\overline{b}_{i,j} + \underline{b}_{i,j}}{2}, \overline{b}_{i,j}\right) \quad \mathcal{N}(d_j, \overline{c}_{i,j}) \quad \mathcal{N}\left(\frac{\overline{b}_{i+1,j} + \underline{b}_{i+1,j}}{2}, \overline{b}_{i+1,j}\right) \quad \mathcal{N}(d_j, \overline{c}_{i+1,j})\right] \quad \text{(eq. 28)}$$

where $\underline{b}_{i,j}$ is a lower bound, $\overline{b}_{i,j}$ and $\overline{c}_{i,j}$ are upper bounds of the parameters and d_j is the center of cluster U_j.

4. Results and discussion

The data collected during the sequential charge and discharge test *(b)* have been used to validate both the designed observers. In the case of the sliding mode observer, the parameters of the model equations (5) and (6) are:

$$A = \begin{bmatrix} 0 & 0 \\ 0 & -1.4 \end{bmatrix}; B = 10^{-3} \cdot \begin{bmatrix} 8.0 \\ 50.45 \end{bmatrix}; C = [0.32 \quad 1]; D = 0.16$$

The parameters of equation (1), that approximate the open circuit voltage in figure 2, are $\varphi(x) = 14.7 - 3.5e^{-2.8x_1}$. The saturation-like function is adopted for the non-linear function $\psi_1(\tilde{y}) = \tanh(\tilde{y})$. The LMI equation (15) is resolved in Matlab using the YALMIP toolbox resulting in matrix F and positive definite matrix P:

$$F = [28.01 \quad 0]; P = \begin{bmatrix} 47.51 & -13.25 \\ -13.25 & 20.42 \end{bmatrix}$$

The linear gain L and the non-linear gain G are calculated from equations (16) and (18):

$$L = \begin{bmatrix} 0.72 \\ 0.47 \end{bmatrix}; G = 10^{-3} \cdot \begin{bmatrix} 24.9 \\ 6.51 \end{bmatrix}$$

The error in the SOC estimation is shown in figure 3. Let us note chattering due to the forced commutation.

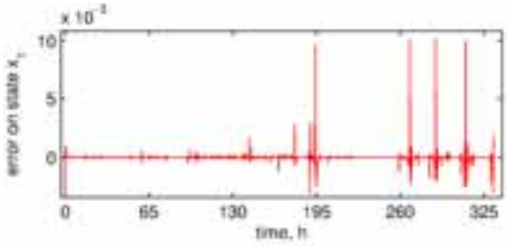

Fig. 3: SOC estimation error

The output error $\tilde{y}(t)$ that is equivalent to the motion onto sliding manifold $\mathcal{S}(\tilde{y}, t) \equiv 0$ is depicted on figure 4. Therefore, the system remains on a sliding manifold.

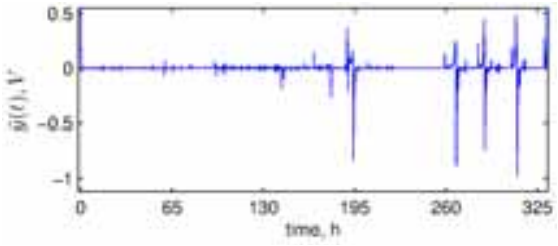

Fig. 4: Output error

In the case of the fuzzy logic observer, the procedure described in Section 3.2 has been used to design and adjust 7 fuzzy rules during 100 iterations of the learning algorithm, which has been implemented in Matlab using the FUZZY toolbox. The set of solution vectors has been limited to 10, with a recombination rate of 40% and a maximum probability of mutation of 0.05. The high-level coding approach has allowed to diminish the length of the solution vector to 28 elements. The traditional 0-1 coding demands a larger number of terms h_j in vector S. The adjusted input membership functions are presented in figures 5.

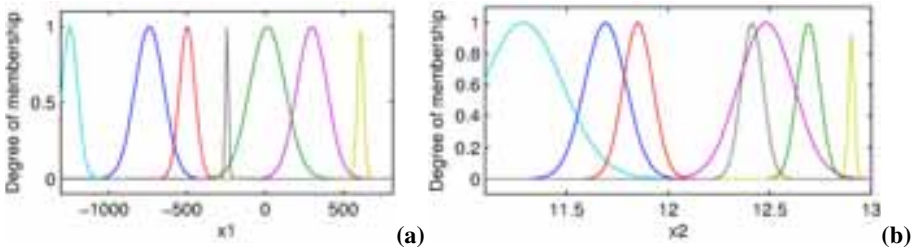

Fig. 5: Membership functions for: (a) input term "Current" and (b) input term "Voltage"

The numerical values are listed in Appendix A.2. The results of the both SOC estimations are presented in figure 6.

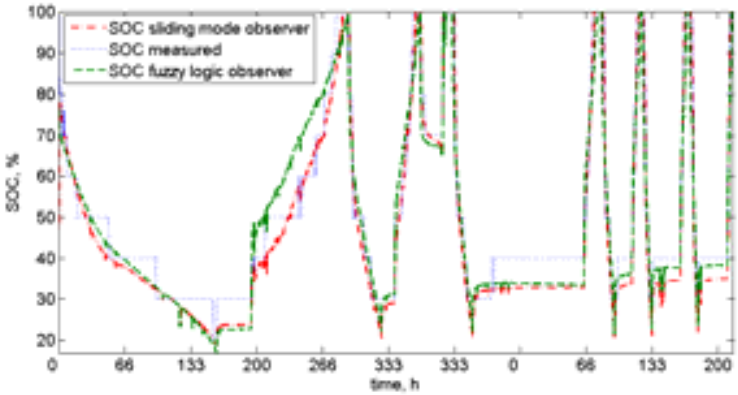

Fig. 6: Comparison of performances of SOC observers

Both designed observers exhibit high capabilities to estimate the SOC. The sliding mode observer has been designed independently of the measured data in test *(b)*. The proposed approach of synthesis exhibits good robustness properties with respect to the modelling imprecision, since the SOC calculated with the sliding mode observer follows the indications of the STECA TAROM 2140 charge regulator.

However, due to the dynamical properties of system (6), the time needed to reach the sliding mode is non-negligible. This time increases with the modelling imprecision, resulting in higher amplitude of the chattering process.

The fuzzy logic observer is free of dynamics and no transient time is needed to achieve the stationary state. However, it is sensitive to the errors accumulated in current integration, according to relation (20). It should be noted that the fuzzy logic observer imitates the behaviour of the charge regulator, since the indications of the charge regulator have been used in the training stage. Therefore, this type of observer is useful to model the behaviour of the energetic plant "storing bank - charge regulator" in order to study issues of different autonomous systems.

5. Conclusion

The developed sliding mode and fuzzy logic observers perform well to estimate the SOC of lead-acid batteries. The first approach allows designing robust observers, which are insensitive to errors and parameter uncertainties and reject any external unpredictable disturbance. However, the chattering in such systems, due to the alterations via application of high-frequency switching control, is a subject to investigate.

The combination of voltage measurement as well as ampere-counting allowed designing a simple and reliable fuzzy logic observer for a time-varying plant with parameter uncertainty and reduced number of available measured values. However, this approach of observer synthesis has its disadvantages - the learning algorithm must have sufficient information with respect to output parameter variations. Hence, it demands rather much time to collect the data.

References

Babuska R., Verbruggen H.B., 1996. An overview of fuzzy modelling for control, Control Engineering Practice, 4 (11), 1593-1606.

Draper N.R., Smith H., 1981. Applied regression analysis, Wiley, New York.

Dunn J.C., 1973. A fuzzy relative of the ISODATA process and its use in detecting compact well-separated clusters, Journal of Cybernetics, 3, 32-57.

Gopikanth M.L., Sathyanarayana S., 1979. Impedance parameters and the state-of-charge. II. Lead acid battery, Journal of Applied Electrochemistry, 9, 369 – 379.

Hu T., Huang B. and Lin Z., 2004. Absolute stability with generalized sector condition, IEEE Transactions On Automatic Control, 49, 535-548.

Jossen A., Piller S., Perrin M., 2001. Methods for state-of-charge determination and their application, Journal of Power Sources, 96, 113-120.

Kim I.-S., 2006. The novel state of charge estimation method for lithium battery using sliding mode observer. Journal of Power Sources, 163, 584-590.

Perruquetti W., Barbot J.P., 2002. Sliding mode control in engineering, Marcel Dekker, Inc., New York.

Piller S., Perrin M., Jossen A., 2001. Methods for state-of-charge determination and their application, Journal Of Power Sources, 96, 113-120.

Rechenberg I., 2000. Case studies in evolutionary experimentation and computation. Computer Methods in Applied Mechanics and Engineering, 186, 125-140.

Rodrigues S., Munichandrajah N., Shukla A.K., 2000. A Review of state of charge indication of batteries by means of A.C. impedance measurements, Journal of Power Sources, 87, 12-20.

Sabatier J., Aoun M., Oustaloup A., Gregoire G., Ragot F., Roy P., 2006. Fractional system identification for lead acid battery state of charge estimation, Signal Processing, 86, 2645-2657.

Salkind A.J., Fennie C., Singh P., Atwater T., Raisner D.E., 1990. Determination of state-of-charge and state-of-health of batteries by fuzzy logic methodology, Journal of Power Sources, 80, 293-300.

Sauer D.U., 1997. Modelling of local conditions in flooded lead/acid batteries in photovoltaic systems, Journal of Power Sources, 64, 181-187.

Singh P., Fennie C., Raisner D., 2004. Fuzzy logic modeling of state-of-charge and available capacity of nickel/metal hybride batteries, Journal Of Power Sources, 136, 322-333.

Soderstrom T., Stoica P., 1988. System Identification, Prentice Hall, London.

Sutano D., Chang H.L., 1995. A new battery model for use with battery storage systems and electric vehicles power systems, IEEE Transactions on Energy Conversation, 4(2).

Utkin V. I., 1978. Sliding modes and their application in variable structure systems. Mir Publishers, Moscow.

Viswanatan V.V., Salkind A.J., Kelley J.J., Ockerman J.B., 1994. Effect of state of charge on impedance spectrum of sealed cells. Part II: Lead acid batteries, Journal of Applied Electrochemistry, 25, 729-739.

Appendix

Appendix A.1. To the explanation of LMI problem formulation

Consider the following LMI:

$$A^T P + P^T A - C^T F - F^T C < 0$$

It can be shown that for $f_1 \in \mathbb{R}^+$, the LMI will have a solution in the matrices F and $P = P^T > 0$. Let assume some values for f_1 and P. Taking into account the numerical values of system's matrices (A, C) from (6), the enlarged relation is written as follows:

$$\begin{bmatrix} 0 & 0 \\ 0 & a_{22} \end{bmatrix} \cdot \begin{bmatrix} p_1 & p_3 \\ p_3 & p_2 \end{bmatrix} + \begin{bmatrix} 0 & 0 \\ 0 & a_{22} \end{bmatrix} \cdot \begin{bmatrix} p_1 & p_3 \\ p_3 & p_2 \end{bmatrix} - \begin{bmatrix} c_1 \\ 1 \end{bmatrix} \cdot \begin{bmatrix} f_1 & 0 \end{bmatrix} - \begin{bmatrix} f \\ 0 \end{bmatrix} \cdot \begin{bmatrix} c_1 & 1 \end{bmatrix} = \begin{bmatrix} -2c_1 f_1 & a_{22} p_3 - f_1 \\ a_{22} p_3 - f_1 & 2a_{22} p_2 \end{bmatrix} < 0$$

Then for every value $f_1 > 0$ and $a_{22} < 0$ the following relations always hold:

$$2c_1 f_1 > 0$$

$$-4c_1 f_1 a_{22} p_2 - (f_1 - a_{22} p_3)^2 > 0$$

Appendix A.2. Numerical values of the fuzzy rules

Tab. 1: Parameters for the output functions

Fuzzy rule	$\boldsymbol{\theta_0}$	$\boldsymbol{\theta_1 \cdot 10^{-2}}$	$\boldsymbol{\theta_2}$
1	-231.18	-2.82	23.49
2	-270.44	-3.96	26.24
3	8.17	-2.53	3.66
4	45.10	-3.44	0.97
5	-349.52	-1.15	33.27
6	-182.23	5.0	18.67
7	-446.21	-1.00	40.78

Tab. 2: Parameters for the input membership functions

Fuzzy rule		x_1, A	x_2, V
1	***b***	91.54	0.102
	c	-742.1	11.69
2	***b***	112.6	0.054
	c	14.07	12.69
3	***b***	49.18	0.073
	c	-499.6	11.85
4	***b***	50.04	0.196
	c	-1252	12.29
5	***b***	95.42	0.135
	c	298.9	12.48
6	***b***	19.46	0.013
	c	61.05	12.90
7	***b***	9.603	0.053
	c	-254.2	12.41